Journal of Hazardous Materials 180 (2010) 466–473

Contents lists available at ScienceDirect

Journal of Hazardous Materials

journal homepage: www.elsevier.com/locate/jhazmat

Photocatalytic performance of ZnO coated tubular reactor

Abdurrahman Akyol [a,*], Mahmut Bayramoglu [b]

[a] Environmental Engineering Department, Gebze Institute of Technology, 41400 Gebze, Turkey
[b] Chemical Engineering Department, Gebze Institute of Technology, 41400 Gebze, Turkey

ARTICLE INFO

Article history:
Received 14 January 2010
Received in revised form 12 April 2010
Accepted 13 April 2010
Available online 18 April 2010

Keywords:
Supported photocatalyst
Zinc oxide
Catalyst preparation
Dipping coating
Ammonium zincate method
Azo dye

ABSTRACT

The recovery of photocatalyst particles constitutes a serious drawback of slurry reactors. Therefore, depositing the catalyst mass on a suitable support without loss of photocatalytic activity is of practical importance. In this study, a chemical deposition method was applied to coat the inner surface of quartz tubes of various diameters with thin ZnO film. The method is economical, energy efficient and easy to apply. ZnO film is mechanically durable and resistant to chemical dissolution. Various physical tests were conducted to characterize the film. ZnO thin film exhibits the crystal wurtzite structure with band gap calculated as 3.24 eV. The film exhibits highly hydrophilic behavior. The average ZnO crystallite size is estimated as 72 nm. SEM analysis shows that the ZnO film has granular morphology with uniform particle size of about 300–400 nm. The film thickness is calculated as 1.41 μm after 20 coating cycles and the increase of the thickness of the thin film per cycle was approximately 70 nm. Photochemical activity tests were performed by measuring photo decolorization rate of a commercial azo dye (Rem Red F3B) solution in tubular reactor and as well as in slurry reactor for comparative purpose. First order rate constants were correlated to principal process parameters. The results showed that thin ZnO film has high photocatalytic activity comparable to that of ZnO powder.

1. Introduction

Semiconductor assisted photocatalysis is one of the mostly investigated advanced oxidation methods for wastewater treatment. The most widespread used photocatalyst is TiO_2 [1–3], but in recent years ZnO with a similar band gap (3.2 eV) has attracted special attention owing to its low cost [4–8]. In spite of the high solid to liquid contact area of catalyst powder slurries, catalyst recycling is the major drawback of slurry reactor. Therefore, deposition of the catalyst on a suitable support is an important subject of research.

The catalyst support and the coating method influence greatly the activity, the technical life and the preparation cost of the catalyst as well as the photoreactor design. The support should be inexpensive, easily accessible and inert in the wastewater medium. Nevertheless, the catalyst should strongly adhere onto support surface to resist against mechanical degradation and photo-corrosion. A literature survey has shown that various materials of different shapes have been proposed as catalyst support among which glass plate [9], glass fiber [10] and glass and ceramic bead [11], aluminum foil sheet [12], plastic fiber-optic cable [13] may be mentioned.

On the other hand, the coating method should be simple, cheap, and convenient for the production at industrial scale and easily adaptable to process control for reproducible catalytic properties. In recent years, various methods have been proposed to prepare supported zinc oxide films, such as thermal oxidation deposition [14–16] electron beam evaporation [17], spray pyrolysis [18–20], different forms of sputtering [21], chemical vapor deposition [22], anodizing [23], heat attachment method [9], sol–gel [24–28] and chemical deposition [29–34]. Among these methods, the chemical deposition from an aqueous solution is a promising method on account of its simplicity and relative low cost.

The aim of this paper was to deposit thin ZnO film on the inner surface of quartz tubes of various diameters by a modified dip-coating method using ammonium zincate solution. The physical characterization of thin film was made by using various techniques. Photocatalytic activity was assessed by investigating the photocatalytic decolorization kinetics of a commercial azo dye, Rem Red F3B (RRF3B), in a differential photoreactor system by monitoring on-line the concentration of the dye solution.

2. Experimental

2.1. Materials

RRF3B (Fig. 1a) was chosen as a commercial azo dye to test the photocatalytic activity. It was supplied by Dystar and used as

* Corresponding author. Tel.: +90 262 605 2140; fax: +90 262 6053205.
E-mail addresses: abdurrahmanakyol@gmail.com, abdakyol@gyte.edu.tr (A. Akyol).

0304-3894/$ – see front matter.
doi:10.1016/j.jhazmat.2010.04.053

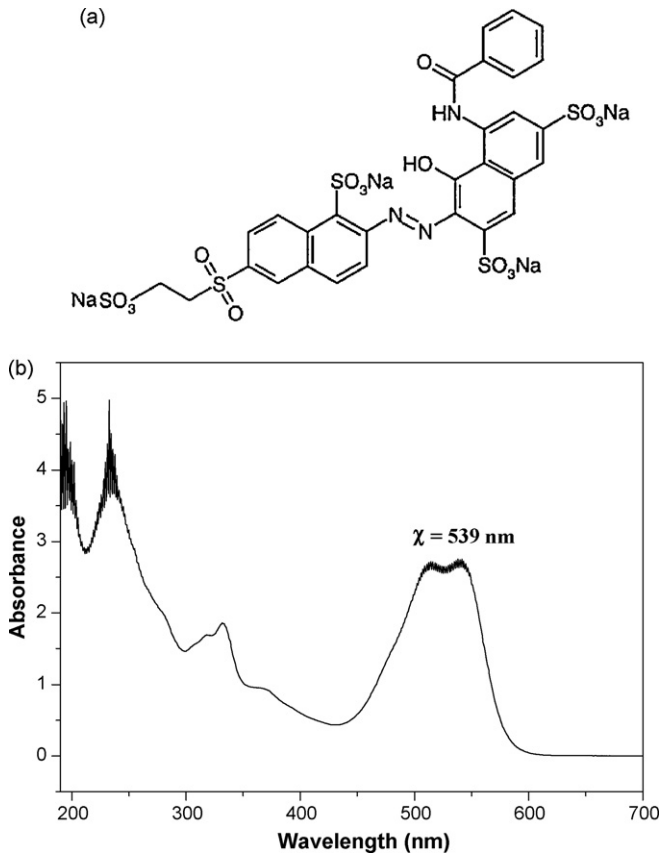

Fig. 1. (a) The structural formula of Rem Red F3B. (b) The UV–visible spectrum of RRF3B.

received. The UV–vis spectrum of this dye in aqueous medium is shown in Fig. 1b. The peak at 539 nm was used to monitor the dye concentration.

2.2. Apparatus

The following tests were made for catalyst film characterization: Micro structural properties by scanning electron microscopy (SEM) (Philips XL30 SFEG), surface roughness by atomic force microscopy (AFM) (Digital Inst.), crystal structures by X-ray diffractometry (XRD) (Rigaku Dmax 2200), Hydrophilicity of the catalyst film by measuring contact angle using KSV 200 Cam. Band gap value of ZnO film was calculated by monochromator (Triax 550). On the other hand, RRF3B concentration was measured using UV/vis-spectrometer (Perkin Elmer, model Lambda 35).

Table 1
ZnO thin film coating process conditions.

Parameter	Unit
Ammonium zincate coating solution concentration	0.2 M
pH of the coating solution	11.0–11.1
Number of coatings	20
Final annealing temperature	300 °C
Annealing period	30 min

2.3. Photoreactor test system

The experimental set-up of the micro photoreactor system is shown in Fig. 2. Standard test conditions are given in Table 1. The tubular quartz reactor is surrounded by six UV-A lamps which predominantly emit at 365 nm (6 W, General Electric F6T5/BLB), positioned so as to ensure homogenous radiation field inside the reactor. Photograph of tubular reactors of various diameters is given in Fig. 3.

Air was blown into the solution tank through a diffuser placed below the impeller tip, in order to maintain the solution saturated with oxygen during the course of the experiment. Prior to irradiation, the dye solution was circulated for 30 min in dark to establish adsorption–desorption equilibrium. Then, RRF3B solution was circulated under UV light for two hours during which the progress of photocatalytic decolorization is monitored by measuring on-line the absorbance of the dye solution in the tank using the fiber-optic probe of UV–vis spectrophotometer. The pH and the temperature of the tank solution were also measured and no significant changes were observed during the experiment. On the other hand, experiments were also conducted with batch slurry reactor using ZnO powder, placed in the same UV illumination system to ensure the same UV irradiation intensity. Liquid samples were withdrawn at 5 min intervals and filtered immediately for spectrophotometric analysis. The experimental results of both reactor systems were used to compare the activities of ZnO thin film and ZnO powder.

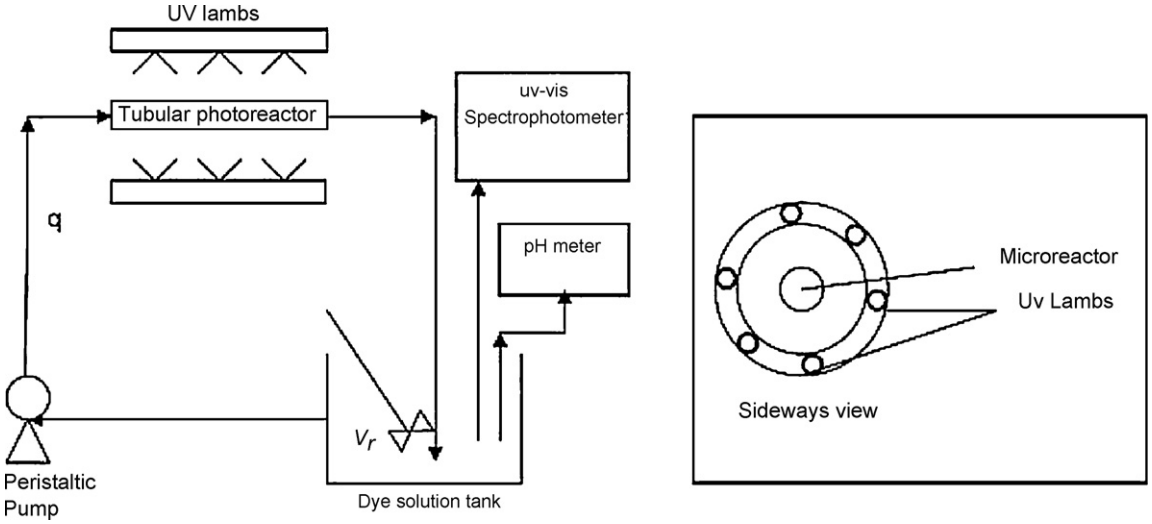

Fig. 2. The experimental set-up of photoreactor system.

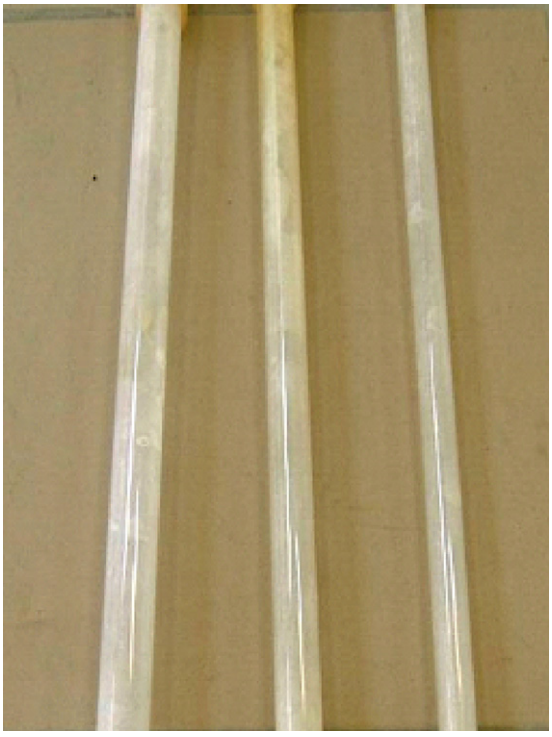

Fig. 3. Photograph of ZnO coated tubular reactors (ϕ 4, 6, 8 mm).

2.4. Photocatalyst preparation

2.4.1. Preparation of ammonium zincate solution

In preparation of ZnO film, zinc acetate was used preferentially as starting material as acetate anion is easily removed during the annealing operation to obtain highly pure ZnO film. Freshly precipitated $Zn(OH)_2$ was prepared by dropping concentrated ammonia solution (25% by weight) into well mixed zinc acetate solution until the final pH became 8

$$Zn(CH_3COO)_2 + 2NH_4OH \leftrightarrow Zn(OH)_2\downarrow + 2CH_3COONH_4 \quad (1)$$

Then, the precipitate was filtered, transferred into another vessel, dispersed in water and while stirred magnetically, concentrated ammonia solution was added rapidly to obtain a clear ammonium zincate solution according to the following reaction:

$$Zn(OH)_2 + 2NH_4OH \leftrightarrow (NH_4)_2ZnO_2 + 2H_2O \quad (2)$$

The final pH of the solution was adjusted to the desired value (11.0 ± 0.1) by evaporating slowly the excess NH_3 by heating the solution. In this way, the purity of the solution was conserved without the addition of foreign ions by acidic neutralization. Finally, Zn concentration of the solution was checked by complexometric analysis to adjust to the desired value if necessary.

2.4.2. Catalyst deposition

The catalyst film formation on support surface occurs through two steps; a dip-coating step where a liquid film is formed by adhesion on the support surface, and a thermal treatment step where liquid film drying and hydrolysis (the reverse of the reaction (1)) occur simultaneously below 100 °C followed by a solid phase transformation of $Zn(OH)_2$ to ZnO above 125 °C.

Deep cleaning of the deposition surface is of great importance to obtain repeatable catalytic properties by ensuring good adherence of the catalyst layer on the support material. For this purpose, a standard cleaning procedure was performed prior to the deposition step; Quartz reactors hold in chromic acid for 2 days were washed amply with distilled water, hold in an ultrasonic bath filled with alcohol solution for 30 min and dried at 105 °C. Moreover, equipments were also cleaned according to the same procedure.

The outline of the coating conditions is given in Table 1. A standard deposition procedure was carried out as follows; quartz glass tube is dipped into 0.2 M ammonium zincate solution, where it was held for 1 min. Later, the glass tube was removed slowly, the outer surface was cleaned and then it was placed into the oven preheated to the selected temperature of 50 °C where it was held for 10 min. In this way, one coating cycle was completed. At the end of 20 coating cycles, the final annealing was accomplished at 300 °C for 10 min to complete the dehydration of $Zn(OH)_2$ and ensure the formation of a strongly adherent ZnO film as well. Other arguments were also taken into account for the selection of the final annealing temperature, as discussed in Section 3.

2.4.3. Zinc analysis

Zn concentration in zincate solution was determined by means of complexometric method. The surface concentration of ZnO was analyzed by atomic absorption spectrophotometer (AAS) using the solution prepared by dissolving the film in HCl solution.

3. Results and discussion

Initially, some coating experiments were performed by depositing ZnO film on microscope slides in order to observe films properties such as film adherence and film homogeneity by naked eye and under optical microscope. Then, various microscopic, structural, optical and tests were conducted to characterize ZnO film coated on glass slides.

3.1. Physical characterization of thin ZnO film

XRD spectra given in Fig. 4a and b reveal that both ZnO thin film and commercial powder ZnO exhibit the same wurtzite (zincite) crystal structure. In addition, the amorphous nature of the ZnO film is easily detected.

The thickness of thin film was estimated by SEM analysis given in Fig. 5. It was calculated as 1.41 μm after 20 coating processes. The thicknesses were also calculated by solving the ZnO film in concentrated acid solution and analyzing ZnO content by AAS and similar results were obtained. From these results, it was concluded that each coating cycle contributes to the film thickness by about 70 nm.

AFM images were taken to discover the structural morphology of ZnO films. The three-dimensional AFM image is given in Fig. 6, from which average ZnO crystallite size was calculated as 72 nm.

Surface hydrophilicity is an important property for an efficient contact of the liquid phase and the catalyst film. This property was evaluated by water contact angle measurements. Fig. 7 shows the water contact measurement for heat treated thin ZnO film. Interestingly, the film exhibits highly hydrophilic behavior (left 36.6°–right 31.0°), as water contact angle is less than 90°. Small angle differences between left and right sides are attributed to the presence of film roughness. The value of water contact angle is less than reported values in the literature [31,35–36]. Meanwhile, its worth to note that the final annealing temperature has important impact on the physical characteristics of the film; the hydrophilicity of the film is inversely related to the annealing temperature as reported by Shinde et al. [31]. Furthermore, the grain size of ZnO increases with increasing heat treatment temperature [27]. Consequently, these considerations restrict the use of high temperatures for the annealing operation.

Band gap value is the principal physical characteristic of semiconductor materials. The theory of optical absorption gives the

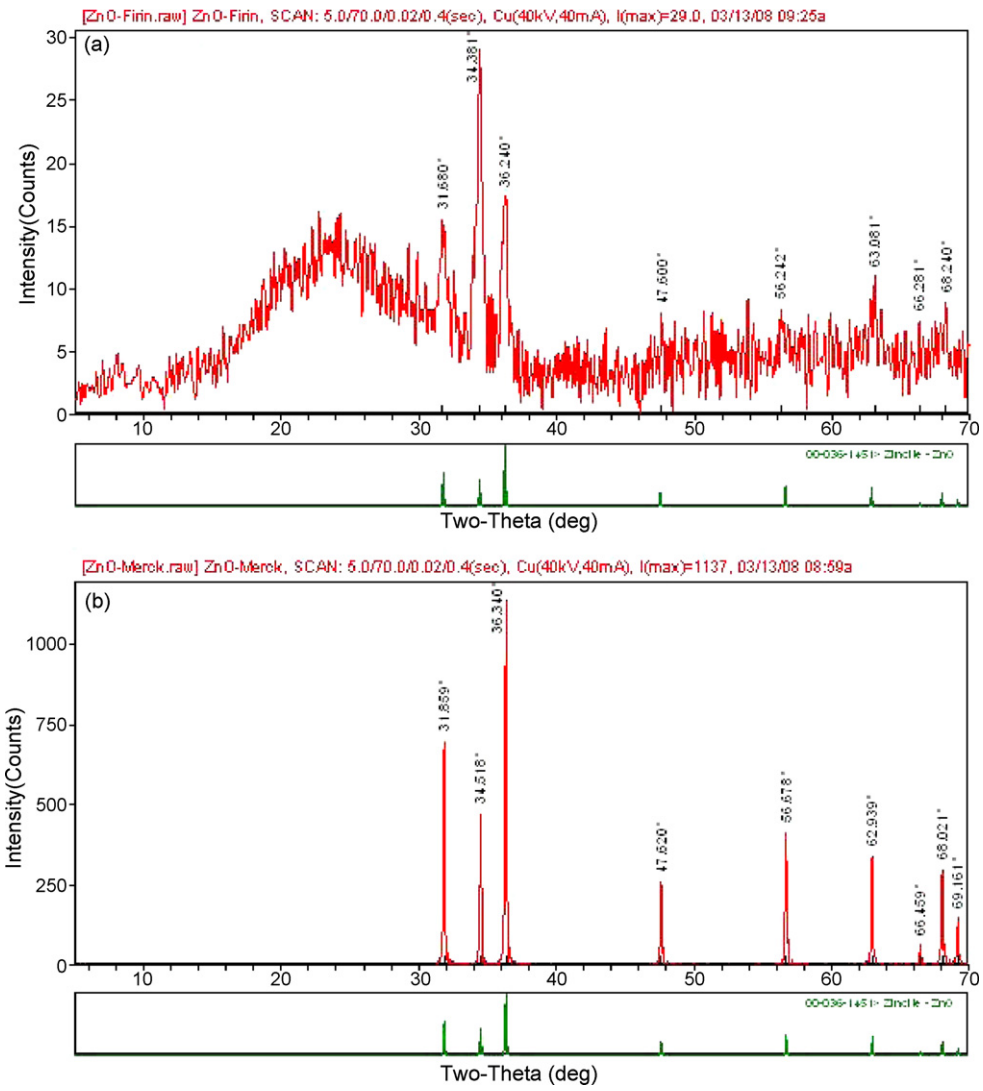

Fig. 4. XRD spectrums of (a) ZnO thin film on glass plate (b) commercial powder ZnO.

relationship (3) between the absorption coefficient α and the photon energy $h\nu$ for direct allowed transition, as in the case of ZnO

$$\alpha h\nu = A(h\nu - E_g)^{n/2} \quad (3)$$

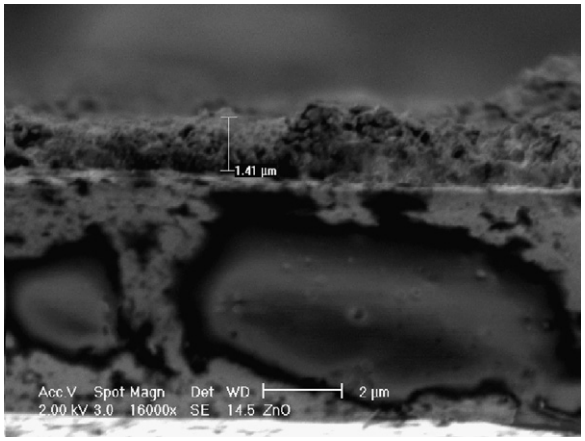

Fig. 5. SEM micrograph of cross-section of microscope slides for thickness of ZnO thin film.

This equation gives the band gap E_g (eV), when the straight portion of $(\alpha h\nu)^2$ against $E(h\nu)$ plot is extrapolated to the point $\alpha = 0$. This is shown in Fig. 8 from which the band gap was calculated as 3.24 eV. Commercial ZnO samples have band gap values between 3.00 and 3.30 eV, and the reported usual value is 3.17 eV. The differences between various band gap values may be due to presence of zinc hydroxide which can remain unconverted during the heat treatment [23], or due to the existence of defect levels after heat treatment, common phenomena observed in chemically deposited thin films [31].

3.2. Photocatalytic activity of ZnO thin film

RRF3B was selected as commonly used commercial textile dye to test the photocatalytic performance. For this purpose, the first order reaction rate constant was used as a measure of the photocatalytic activity, since photocatalytic reactions comply generally with pseudo first order kinetic model:

$$-\ln(C/C_0) = k\,t_f \quad (4)$$

where k is the rate constant (h^{-1}), t_f is the photocatalytic reaction time (h) calculated from the processing time t, according to Eq. (5)

$$t_f = t\ (V_t/V_r) \quad (5)$$

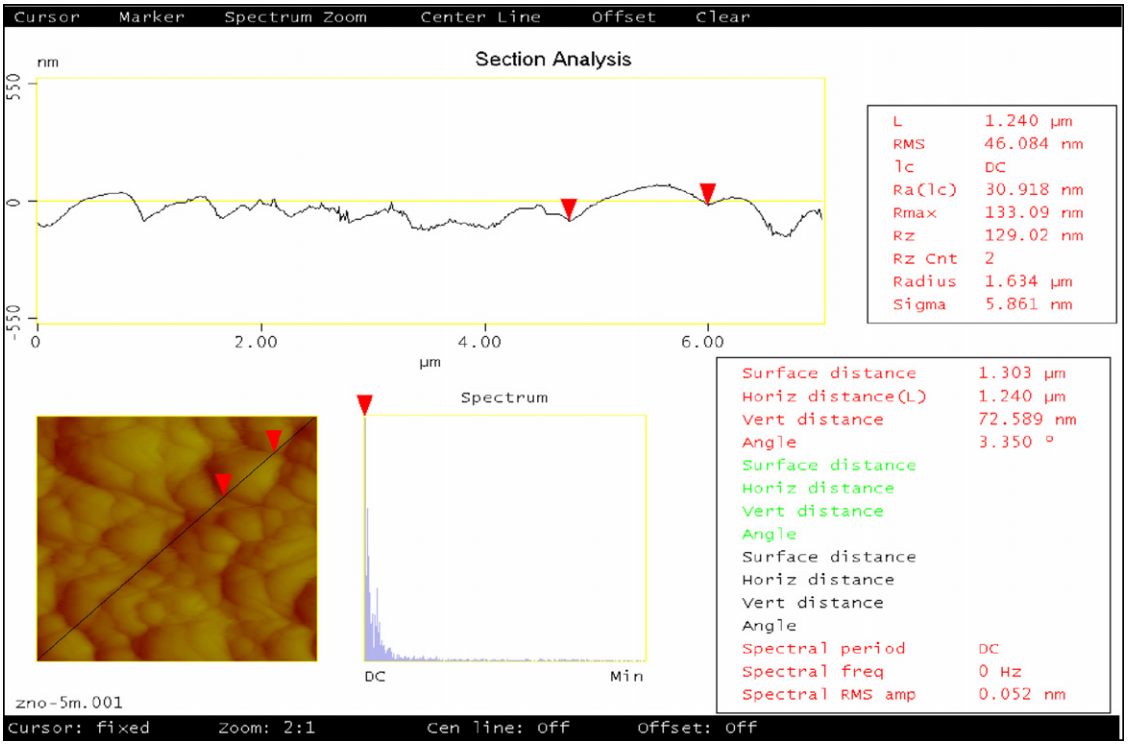

Fig. 6. Atomic force microscope (AFM) images of ZnO thin film.

where V_t is the total liquid volume in the system (dm^3), V_r is the active liquid volume in the reactor in contact with UV radiation field.

In the calculation of the rate constants by means of linear regression, on-line absorbance data comprising approximately 100–300 samples was used. On the other hand, in slurry reactor experiments, at least 10 kinetic data were used for this purpose. To test the reproducibility of the rate constant values, the relative experimental error was estimated using the results of three replicate experiments and it was calculated as 5%, which is of acceptable

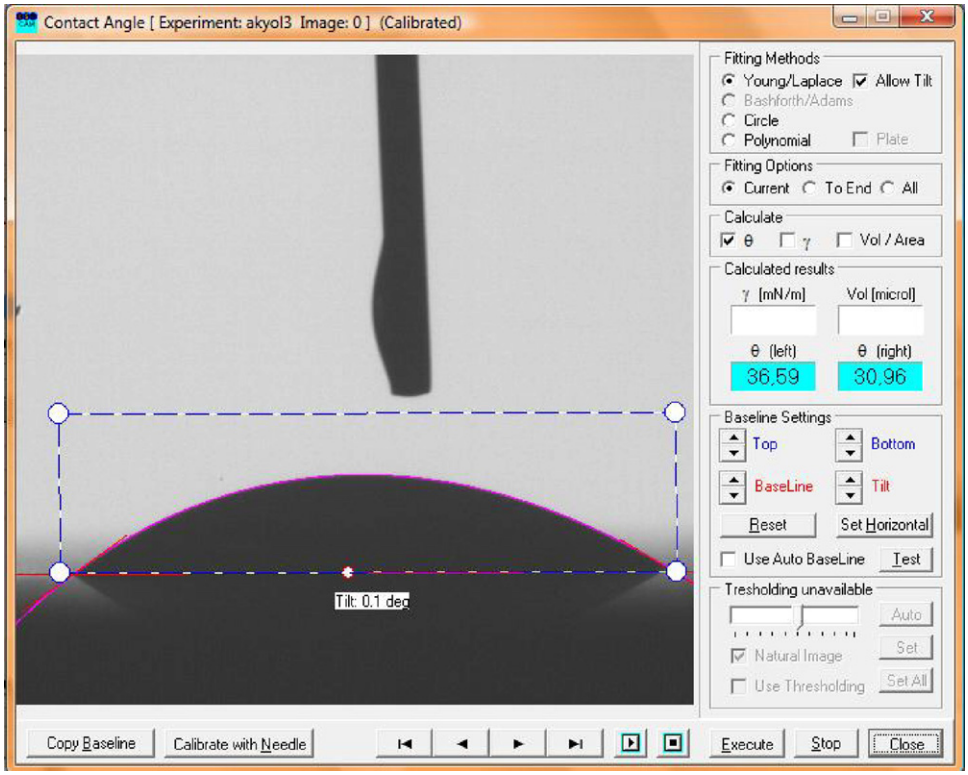

Fig. 7. Contact angle calculation of ZnO thin film.

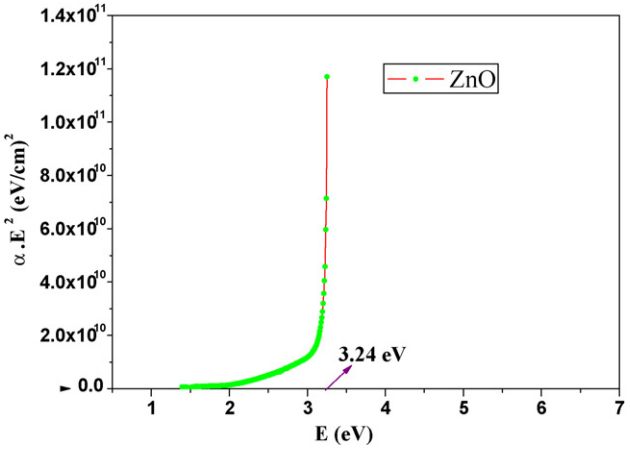

Fig. 8. Band gap calculation of ZnO thin film (αE^2 and E (eV)).

level when the complexity of various physical-chemical processes occurring during the whole process is taken into account.

On the other hand, photocatalytic rate depends on diverse process parameters such as; initial organic dye concentration C_0 (mmol dm^{-3}), volumetric photon absorption velocity I (mW dm^{-3}), volumetric catalyst loading m (mg dm^{-3}). The rate constant was correlated to these process parameters according to the power law model (Eq. (6)) as usually applied for this purpose [5]:

$$k = a\ m^b\, C_0^c\, I^d \tag{6}$$

The model parameters, a, b, c, d were determined by linear regression analysis after suitable logarithmic transformations.

The solution pH, air flow and temperature were held constant at 6.5, 200 cm^3 min^{-1} and 25 °C respectively in all experiments. The same parameter ranges applied in the whole kinetic study are as follows:

Variable ranges: C_0: 0.027–0.133 mM; I: 176–528 mW dm^{-3}

Base experimental conditions are as follows; C_0 = 0.160 mM, I = 528 mW dm^{-3}.

3.2.1. Kinetic modeling with powder ZnO photocatalyst

In slurry reactor experiments, the stirring rate was held constant at 300 rpm. The base catalyst loading value was 1500 mg dm^{-3}, which was investigated between 35 and 3000 mg dm^{-3}.

The regression analysis according to Eq. (6) gave the following results:

$$k_{pow} = 1.63 \times 10^{-5}\, m^{0.80}\, C_0^{-1.69}\, I^{0.51} \quad (R^2 = 0.982,\ s = 0.068) \tag{7}$$

where R^2 is the squared correlation coefficient and s is the root mean square error. The fit between model and experimental k values is shown in Fig. 9. Exponent of I is approximately equal to 0.5, as found frequently. Furthermore, Exponent of C_0, −1.69, which is quite higher than the usual value −1, results primarily from the reduction of the path length of photons entering the solution by increasing dye concentration, according to the Lambert–Beer law.

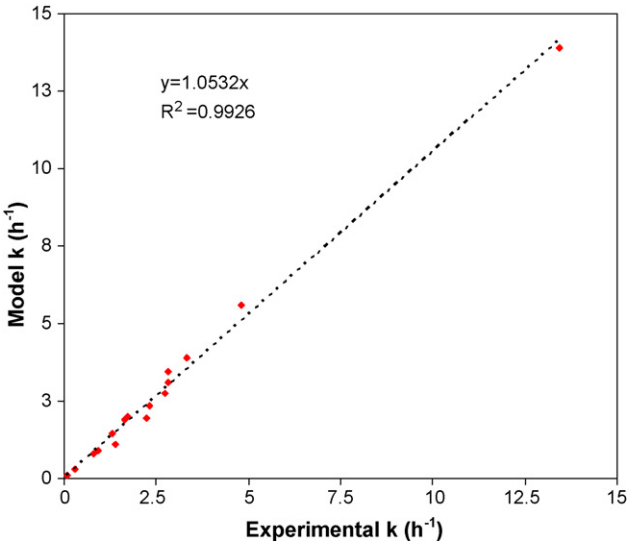

Fig. 9. Fit between model and experimental rate constants values with ZnO powder.

Table 2
Experimental conditions of the reactor system.

Parameter	Value
Quartz tube reactor diameters	ϕ 6–12 mm
Quartz tube reactor length	180 mm
Air flow	200 cm^3 min^{-1}
Total dye solution volume	100 cm^3
Liquid circulation velocity	225 cm^3 min^{-1}

3.2.2. Kinetic modeling with ZnO coated tubular reactors

Quartz tubes of various diameters namely, 4, 6, 8, 10 and 12 mm were coated with thin ZnO film. Photocatalytic activities of tubular reactors were tested as function of initial dye concentration, volumetric photon absorption rate and tube diameter. Constant process conditions applied for kinetic study are given in Table 2. Liquid recycle flow rate was adjusted to ensure similar flow (hydrodynamic) conditions for each tube diameter. Reynolds number was adjusted near to 1000 to prevent mechanic corrosion of thin film by turbulent flow.

According to Table 3, it is seen that two important properties of the catalyst layer namely, superficial catalyst loading S_k and film thickness, are both independent of tube diameter within experimental error. This also shows that the coating method was applied successfully on tubes of various diameters. On the other hand, for surface driven heterogeneous photocatalysis, a linear dependence is expected between the rate constant and specific surface area, but a sigmoid curve was obtained experimentally as seen in Fig. 10, reflecting the complex nature of photocatalytic process involving various series and parallel steps such as mass transfer to or from catalyst surface, chemical surface reactions, photonic adsorption and related electronic phenomena. Detailed mechanistic models encompassing all the aspects of photocatalytic processes are given in various reviews [37–38]. Meanwhile, the results demonstrate that narrower reactor is more beneficial for an efficient use of

Table 3
Specific properties of tubular reactors.

Tubular reactor diameter (mm)	V (cm^3)	Catalytic surface/reactor volume (S_v) (cm^2 cm^{-3})	S_k (mg cm^{-2})	Thickness of ZnO thin film (μm)	k (h^{-1})
4	2.51	9.8	0.87	1.55	5.50
6	5.65	6.6	0.89	1.58	4.80
8	10.05	5.0	0.83	1.47	2.06
10	15.70	4.0	0.77	1.37	1.24
12	22.61	3.4	0.84	1.49	0.21

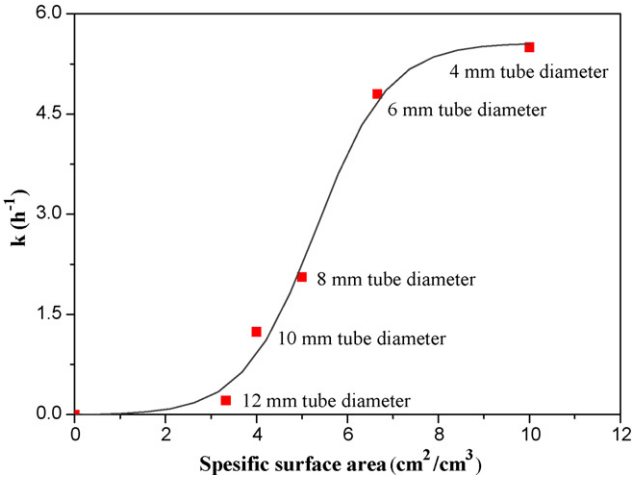

Fig. 10. Experimental rate constants as function of specific surface area of tubular reactor.

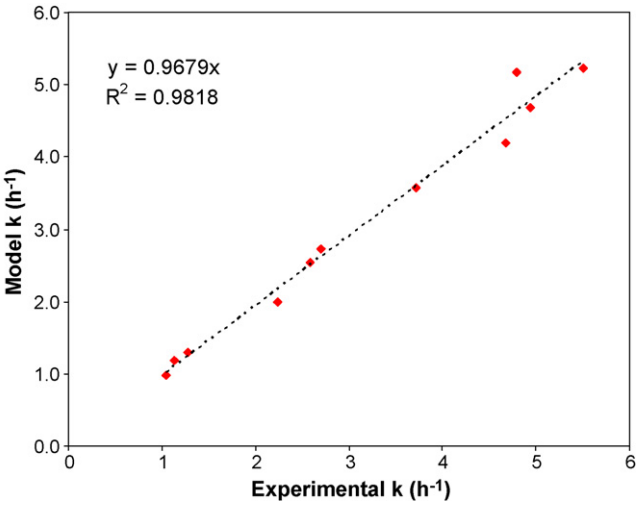

Fig. 12. Fit between model and experimental rate constants values with tubular reactor.

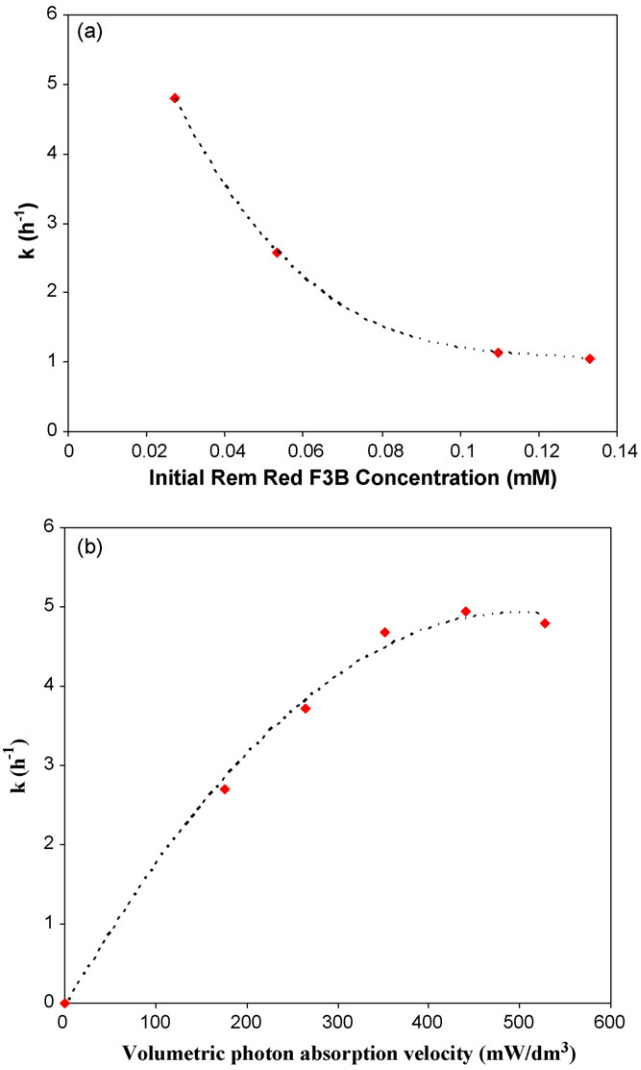

Fig. 11. On photocatalytic decolorization of RRF3B with 6 mm tube reactor. (a) Effect of initial dye concentration the rate constant (b) effect of volumetric photon absorption velocity the rate constant.

catalyst film deposited on the inner surface of the reactor. Larger reactors may be operated as "falling film reactor".

For 6 mm tubular reactor, the dependence of the rate constant on initial RRF3B concentration and volumetric photon absorption velocity are shown in Fig. 11a and b respectively. Linear regression analysis gave the following results:

$$k_{film} = 3.08 \times 10^{-3}\, C_0^{-1.05}\, I^{0.58} \quad (R^2 = 0.989,\ s = 0.031) \tag{8}$$

The fit between model and experimental k values is shown Fig. 12. On the other hand, when Eqs. (7) and (8) are compared, it is seen that the powers of the dye concentration and light intensity terms differ for thin film and powder catalyst: In the case of thin film, the rate constant is less sensitive to initial dye concentration, and more sensitive to light intensity.

Dividing Eq. (7) by Eq. (8), the ratio of the rate constants, or equivalently the ratio of the activities is obtained

$$\frac{k_{pow}}{k_{film}} = \frac{0.0053\ m^{0.80}}{C_0^{0.64}\, I^{0.7}} \tag{9}$$

The following numerical example may be given for illustrative purpose: according to Eq. (9), for $C_0 = 0.01$ mM and $I = 176$ mW dm^{-3}, the activity of the ZnO film is equal to the activity of ZnO powder in a slurry of 1620 mg dm^{-3} density. On the other hand, based on particle size distribution analysis, the specific optic surface area of ZnO powder was calculated as 3.47 m^2 g^{-1}. Thus, total optic surface area of catalyst slurry of 1620 mg dm^{-3} density is about 56.2 cm^2 cm^{-3} of slurry volume, while the corresponding S_v value is only 6.6 cm^2 cm^{-3} of reactor volume; in other words, catalyst mass is 8.5 times more efficiently used in thin film coated tube reactor than slurry reactor to achieve the same photocatalytic activity.

4. Conclusion

A chemical deposition method was applied to coat various quartz tubes with ZnO thin film through two steps; a dipping step in an ammonium zincate solution to form a liquid film on support surface and a thermal treatment step for the formation of ZnO film. The method uses low cost inorganic Zn compound dissolved in ammonia solution. It is energy efficient since it does not require high annealing temperature. ZnO thin film has a wurtzite crystal structure with band gap calculated as 3.24 eV. It exhibits highly hydrophilic behavior. The average ZnO crystallite size was estimated as 72 nm. The thickness of thin film estimated by SEM

microgram analysis was calculated as 1.41 μm after 20 coating processes. The dependences of the first order rate constant to initial dye concentration and light intensity are different from those of ZnO powder; the rate constant is less sensitive to initial dye concentration and more sensitive to light intensity, which demonstrates a more efficient use of light photons. The results showed that thin ZnO film deposited on the inner surfaces of the tubular reactor has comparable photocatalytic activity to that of ZnO powder and catalyst mass is more efficiently used in thin film coated tube reactor than slurry reactor to achieve the same photocatalytic activity.

Acknowledgements

This research work is a part of the project which is supported by TUBITAK—the Scientific and Technological Research Council of Turkey – under contract number MAG-104M411.

References

[1] C. Reyes, J. Fernandez, J. Freer, M.A. Mondaca, C. Zaror, S. Malato, H.D. Mansilla, Degradation and inactivation of tetracycline by TiO_2 photocatalysis, J. Photochem. Photobiol. A. 184 (2006) 141–146.
[2] S.P. Cho, S.C. Hong, S.-I. Hong, Photocatalytic degradation of the landfill leachate containing refractory matters and nitrogen compounds, Appl. Catal. B-Environ. 39 (2002) 125–133.
[3] M. Vautier, C. Guillard, J.-M. Herrmann, Photocatalytic degradation of dyes in water: case study of Indigo and Indigo Carmine, J. Catal. 201 (2001) 46–59.
[4] A. Akyol, M. Bayramoglu, Photocatalytic degradation of Remazol Red F3B using ZnO catalyst, J. Hazard. Mater. 124 (2005) 241–246.
[5] H.C. Yatmaz, A. Akyol, M. Bayramoglu, Kinetics of the photocatalytic decolorization of an Azo reactive dye in aqueous ZnO suspensions, Ind. Eng. Chem. Res. 43 (2004) 6035–6039.
[6] M. Zhang, T. An, X. Hu, C. Wang, G. Sheng, J. Fu, Preparation and photocatalytic properties of a nanometer ZnO–SnO_2 coupled oxide, Appl. Catal. A-Gen. 260 (2004) 215–222.
[7] A. Akyol, H.C. Yatmaz, M. Bayramoglu, Photocatalytic decolorization of Remazol Red RR in aqueous ZnO suspensions, Appl. Catal. B-Environ. 54 (2004) 19–24.
[8] A. Akyol, M. Bayramoglu, The degradation of an azo dye in a batch slurry photocatalytic reactor, Chem. Eng. Process 47 (2008) 2150–2156.
[9] M.A. Behnajady, N. Modirshahla, N. Daneshvar, M. Rabbani, Photocatalytic degradation of C.I. Acid Red 27 by immobilized ZnO on glass plates in continuous-mode, J. Hazard. Mater. 140 (2007) 257–263.
[10] C.H. Aoa, S.C. Lee, C.Y. Jimmy, Photocatalyst TiO_2 supported on glass fiber for indoor air purification: effect of NO on the photodegradation of CO and NO_2, J. Photochem. Photobiol. A 156 (2003) 171–177.
[11] A. Akyol, M. Bayramoglu, Preparation and characterization of supported ZnO photocatalyst by zincate method, J. Hazard. Mater. 175 (2010) 484–491.
[12] F. Peng, H. Wang, H. Yu, S. Chen, Preparation of aluminum foil-supported nanosized ZnO thin films and its photocatalytic degradation to phenol under visible light irradiation, Mater. Res. Bull. 41 (2006) 2123–2129.
[13] H. Jooa, H. Jeong, M. Jeon, I. Moon, The use of plastic optical fibers in photocatalysis of trichloroethylene, Sol. Energy Mater. Sol. Cells 79 (2003) 93–101.
[14] O.A. Fouad, A.A. Ismail, Z.I. Zaki, R.M. Mohamed, Zinc oxide thin films prepared by thermal evaporation deposition and its photocatalytic activity, Appl. Catal. B-Environ. 62 (2006) 144–149.
[15] R.K. Gupta, N. Shridhar, M. Katiyar, Structure of ZnO films prepared by oxidation of metallic Zinc, Mater. Sci. Semicond. Process. 5 (2002) 11–15.
[16] Y.G. Wang, S.P. Lau, H.W. Lee, S.F. Yu, B.K. Tay, X.H. Zhang, H.H. Hng, Photoluminescence study of ZnO films prepared by thermal oxidation of Zn metallic films in air, J. Appl. Phys. 94 (2003) 354–358.
[17] Y. Leprince-Wang, K. Yu-Zhang, V.N. Van, D. Souche, J. Rivory, Correlation between microstructure and the optical properties of TiO_2 thin films prepared on different substrates, Thin Solid Films 307 (1997) 38–42.
[18] C. Natarajan, N. Fukunaga, G. Nogami, Titanium dioxide thin film deposited by spray pyrolysis of aqueous solution, Thin Solid Films 322 (1998) 6–8.
[19] W.A. Badawy, Preparation, electrochemical, photoelectrochemical and solid-state characteristics of indium-incorporated TiO_2 thin films for solar cell fabrication, J. Mater. Sci. 32 (1997) 4979–4984.
[20] M. Miki-Yoshida, V. Collins-Martinez, P. Amezaga-Madrid, A. Aguilar-Elguezabal, Thin films of photocatalytic TiO_2 and ZnO deposited inside a tubing by spray pyrolysis, Thin Solid Films 419 (2002) 60–64.
[21] M. Stromme, A. Gutarra, G.A. Niklasson, C.G. Granqvist, Impedance spectroscopy on lithiated ti oxide and ti oxyfluoride thin films, J. Appl. Phys. 79 (1996) 3749–3757.
[22] V. Gauthier, S. Bourgeosis, P. Sibillot, M. Maglione, M. Sacillotti, Growth and characterization of AP-MOCVD iron doped titanium dioxide thin films, Thin Solid Films 340 (1999) 175–182.
[23] Y. Yamaguchi, M. Yamazaki, S. Yoshihara, T. Shirakashi, Photocatalytic ZnO films prepared by anodizing, J. Electroanal. Chem. 442 (1998) 1–3.
[24] B. Pal, M. Sharon, Enhanced photocatalytic activity of highly porous ZnO thin films prepared by sol–gel process, Mater. Chem. Phys. 76 (2002) 82–87.
[25] J.A. Navio, G. Colon, M. Macias, C. Real, M.I. Litter, Iron-doped titania semiconductor powders prepared by a sol–gel method. Part I: synthesis and characterization, Appl. Catal. A-Gen. 177 (1999) 111–120.
[26] Y.H. Cheng, L.K. Teh, Y.Y. Tay, H.S. Park, C.C. Wong, S. Li, Coating process of ZnO thin film on macroporous silica periodic array, Thin Solid Films 504 (2006) 41–44.
[27] Z. Jiwei, Z. Liangying, Y. Xi, The dielectric properties and optical propagation loss of *c*-axis oriented ZnO thin films deposited by sol–gel process, Ceram. Int. 26 (2000) 883–885.
[28] D. Bao, H. Gu, A. Kuang, Sol–gel derived *c*-axis oriented ZnO thin films, Thin Solid Films 312 (1998) 37–39.
[29] P. Mitra, J. Khan, Chemical deposition of ZnO films from ammonium zincate bath, Mater. Chem. Phys. 98 (2006) 279–284.
[30] V.R. Shinde, T.P. Gujar, C.D. Lokhanda, Studies on growth of ZnO thin films by a novel chemical method, Sol. Energy Mater. Sol. Cells 91 (2007) 1055–1061.
[31] V.R. Shinde, C.D. Lokhanda, R.S. Mane, S.H. Han, Hydrophobic and textured ZnO films deposited by chemical bath deposition: annealing effect, Appl. Surf. Sci. 245 (2005) 407–413.
[32] A.E. Jimenez-Gonzailez, Modification of ZnO thin films by Ni, Cu, and Cd doping, J. Solid State Chem. 128 (1997) 176–180.
[33] A.E. Jimenez-Gonzailez, P.K. Nair, Photosensitive ZnO thin films prepared by the chemical deposition method SILAR, Semicond. Sci. Technol. 10 (1995) 1277–1281.
[34] K. Ramamoorthy, M. Arivanandhan, K. Sankaranarayanan, C. Sanjeeviraja, Highly textured ZnO thin films: a novel economical preparation and approachment for optical devices, UV lasers and green LEDs, Mater. Chem. Phys. 85 (2004) 257–262.
[35] R.-D. Sun, A. Nakajima, A. Fujishima, T. Watanabe, K. Hashimoto, Photoinduced surface wettability conversion of ZnO and TiO_2 thin films, J. Phys. Chem. B 105 (2001) 1984–1990.
[36] M. Li, J. Zhai, H. Liu, Y. Song, L. Jiang, D. Zhu, Electrochemical deposition of conductive superhydrophobic zinc oxide thin films, J. Phys. Chem. B 107 (2003) 9954–9957.
[37] A. Mills, R.H. Davies, D. Worsley, Water-purification by semiconductor photocatalysis, Chem. Soc. Rev. 22 (1993) 417–425.
[38] O. Legrini, E. Oliveros, A.M. Braun, Photochemical processes for water treatment, Chem. Rev. 93 (1993) 671–698.